18TH WORLD CONFERENCE ON EARTHQUAKE ENGINEERING
WCEE2024
MILAN

MILAN, ITALY
30TH JUNE - 5TH JULY 2024

www.wcee2024.it

AUTOMATED DEVELOPMENT OF SEISMIC FRAGILITIES AND FINITE ELEMENT MODELS FOR NONDUCTILE REINFORCED CONCRETE BUILDINGS

Peng-Yu Chen[1], Nikolaos Lesgidis[2], Anastasios Sextos[3] & Ertugrul Taciroglu[4]

[1] Dept. of. Civil Engineering, National Central University, Taoyuan, Taiwan, sam75782008@g.ncu.edu.tw

[2] Deep Excavation LLC, New York, USA

[3] Dept. of Civil Engineering, University of Bristol, Bristol, UK

[4] Dept. of Civil & Env. Engineering, University of California, Los Angeles, USA

Abstract: The nonductile reinforced concrete building (NDRCB) stock—typically, pre-1974 structures in the United States—is a well-known high-risk group, given the lack of seismic design provisions at the code enforced at that time. It is estimated that there are approximately 1,500 NDRCBs in Los Angeles, and their owners are currently required to choose between demolition and seismic retrofitting. Given that both options are associated with significant costs and broader social implications, the potential risk of significant losses will persist as it will take decades to fulfill these requirements. This study establishes an automated method for evaluating the seismic risk of nonductile moment-resisting frames to accelerate and facilitate rapid assessment of regional risks. The proposed method uses building metadata and era-specific seismic design guidelines to develop archetypal models in OpenSees. These models are verified through nonlinear quasi-static cyclic and dynamic analyses against prior analytical/numerical studies and specimen tests. Fragility curves for discrete damage states are also developed through a probabilistic seismic demand model, and the method is evaluated using sensitivity analyses of several building configurations and properties considering soil-structural interaction effects. The most suitable seismic intensity measures to quantify the seismic damage levels of NDRCB frames are also investigated. The application of the proposed method to the estimation of the residual functionality for NDRCBs in Los Angeles is also presented in order to demonstrate its potential utility in large-scale resilience assessment. The proposed method can provide a rapid yet rigorous assessment of potential seismic losses of NDRCB structures and support decision-making by governing bodies responsible for addressing disproportionate risks from substandard structures in highly seismic regions.

1 Introduction

Seismic vulnerabilities of NDRCBs were evident in past earthquakes, including Northridge (1994); Kobe, Japan (1995); Chi-Chi, Taiwan (1999); and L'Aquila, Italy (2009); Kahramanmaras, Turkey (2023). The poor performance of this building type is primarily caused by the lack of confinement to the concrete cores of beams, columns, joints, and walls, which results in brittle failures of structural components. Previous studies have undertaken numerous efforts to identify and generate reliable databases of NDRCBs in California to understand the risks posed by these collapse-prone buildings and develop countermeasures. The Concrete Coalition identified 20,000 to 23,000 NDRCBs in California, including residential, commercial, and public (e.g., school) buildings (Comartin et al., 2011). The investigation took three years to assemble a variety of data sources ranging from county assessor's files to satellite images. Site surveys were also conducted to corroborate data collected from multiple sources. With the experience of Concrete Coalition, a case study inventory of the City of Los Angeles was then conducted, and approximately 1,500 NDRCBs were identified (Anagnos et al., 2008). The inventory has been compiled using more than 15 data sources, and the attributes

include location, structural type, year built, number of stories, total size in square footage, and building usage. To address the seismic loss and the mitigation priorities, Anagnos et al. (2016) broke down the inventory into groups representing common construction typologies and estimated the loss for scenario events. Cost-benefit analyses were also carried out to examine various retrofit approaches, contributing to Los Angeles' seismic ordinance, which mandates retrofitting or demolition of NDRCBs. Because the fulfillment of these ordinances will last for decades, more than one thousand NDRCBs are still pending assessment to determine their compliance with this ordinance.

In addition to the potential risk posed by NDRCBs, the expected repair time for them to recover the corresponding functionality is an important index to quantify the city's resilience. In recent years, the increasing frequency of extreme natural disasters has prompted nations worldwide to prioritize cultivating resilient cities. In particular, seismic resilience, a term that refers to the ability of a single building or a cluster of structures to withstand and recover from earthquake hazards, has become of utmost importance. The resilience of a building in the face of an earthquake is primarily determined by its seismic performance. Specifically, the damage state, collapse probability, residual capacity, and functionality are the most crucial indices to quantify resilience (Castillo et al., 2022).

Given the increasing demands on large-scale assessments of seismic response and resilience, an open-source workflow that integrates inventory data, numerical modeling, and seismic risk assessment of NDRCBs is being developed in this paper. The critical elements of the presented work are (1) the construction of relatively detailed and computationally efficient models to approximate as-built structures based on geometric information and material properties and (2) the effective execution of many nonlinear dynamic analyses to construct fragility functions for seismic risk assessment. Such a workflow can then be used to estimate the potential damage and repair time by following the state-of-the-practice probabilistic seismic assessment methodology FEMA P-58 (ATC, 2012). It can further aid engineers and policy-makers by providing them with a relatively more detailed and accurate assessment of seismic risk at regional scales.

2 Numerical Model

2.1 Automated modeling of NDRCBs

Prior studies have underlined the accuracy and efficiency of using archetypal buildings to simulate the NDRCBs (Liel et al., 2011, 2012, 2013), where the key to the numerical simulation of NDRCB frames is to capture their lateral capacities and strength and stiffness degradation behaviors under cyclic loading. Scaling up detailed and expert-level modeling of NDRCBs to a regional inventory is challenging. As such, this study aims to automate model generation, achieved herein by implementing a “design” procedure that requires only the basic metadata (e.g., the number of floors, square footage, etc.) to produce an analytical model that can approximate the as-built structure. In the said design procedure, the era-specific building code, the 1967 Uniform Building Code (UBC), is the primary means for developing an approximate structural model.

In UBC, the required lateral force depends on the base shear V calculated as $V=CKW$. In this approximation, W is the weight of the building, and C is the base shear coefficient determined by

$$C = \frac{0.05}{\sqrt[3]{T}} \tag{1}$$

which, in turn, depends on the fundamental period of the structure and should not be larger than 0.1. The term K denotes the horizontal force factor and varies from 0.67 (ductile) to 1.33 ($K=1$ for nonductile frames). In the proposed method, W was calculated based on the floor area, floor weight (including both dead and live loads), and the number of floors. The dead load was assumed to be 175 psf, and the live load was assigned based on the usage specified in UBC. Two types of archetypal frames were developed following the prior studies, and their tributary areas are illustrated in Figure 1, which was used for determining the weight contributing to the lateral forces. Finally, C was calculated based on the structural period, which was assumed to be 0.1 times the total number of floors (ASCE, 2013), and K was fixed to 1 for all NDRCB frames. Once the base shear was obtained, the distributed lateral forces could be calculated using Equations 2 to 4, wherein F_t and F_i represent the lateral forces applied to the roof and i^{th} floor; h_x, w_x, h_n, and w_n are the height and floor weight at the x^{th} floor and roof in the respective pairs; D_n is the plane dimension of the roof.

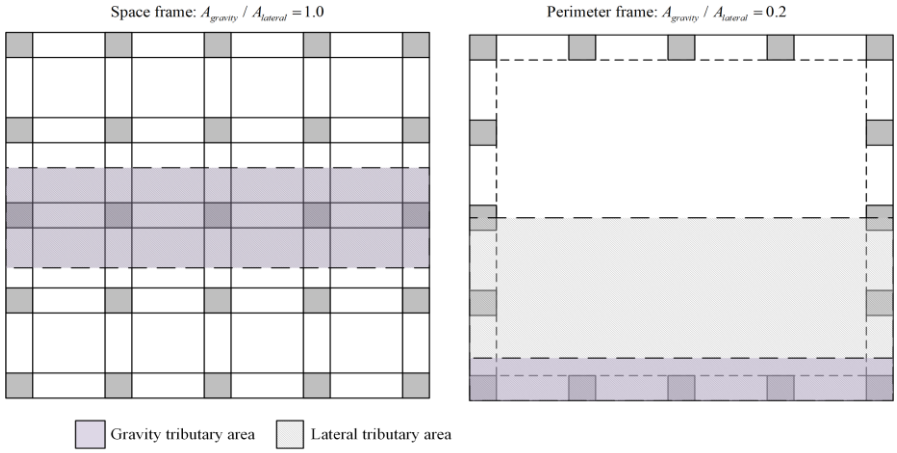

Figure 1. Planview and ratio of gravity to lateral tributary areas of two archetype structures.

$$V = F_t + \sum_{i=1}^{N} F_i \tag{2}$$

$$F_t = 0.004V\left(\frac{h_n}{D_n}\right)^2 \tag{3}$$

$$F_x = \frac{(V - F_t)w_x F_x}{\sum_{i=1}^{N} w_i h_i} \tag{4}$$

The load combination required by UBC was used to analyze the maximum and second-largest internal forces and check the component capacity on the first floor and typical floors (2nd and above). The “Ultimate Strength Design” method and the detailing requirements specified in Sections 2615, 2616, 2617, and 2619 in the UBC are applied to the archetypal structures.

In the proposed design procedure, six archetypal frames were selected from Liel et al. (2011) to develop a preliminary OpenSees model with assigned/provided building configurations (i.e., number of floors, floor height, floor area, number of spans, etc.) and to conduct static analysis to obtain the demand for the components. The observed forces can be used with the preliminary model to check the component capacities. If the capacity is insufficient, the proposed algorithm iteratively modifies the reinforcement details (the number and size of rebars) and member dimensions (depth and width). Although the algorithm displays robust convergence to a final design, the outcome of the design cannot necessarily reproduce the decisions made by the original designers. Nevertheless, it generates realistic estimates of unavailable information (e.g., dimensions of columns and beams, reinforcement ratios, and rebar spacing). Once and if the design algorithm converges, the generated model is guaranteed to meet the minimum requirements of UBC.

Once the design procedure is completed, the proposed method automatically outputs OpenSees’ model according to the element definitions summarized in Figure 2. Elastic beam-column elements are preferred over fiber-based beam-column elements when creating the model to reduce the computational cost. For the same reason, the brittle failure mode considered here only captures the shear and axial failure in the columns but does not capture the joint-shear failure. Finally, the beams' shear and axial failure modes are omitted because UBC specifications typically result in strong-beam weak-column systems.

The concentrated plastic hinge was used in the proposed model to simulate the strength deterioration. The material model used for defining its response is the Modified Ibarra-Medina-Krawinkler model with a peak-oriented hysteretic response (Ibarra et al., 2004; Lignos et al., 2013). Six parameters are required to control the monotonic and cyclic behavior, namely, the elastic stiffness K_e, yielding moment M_y, capping to yielding moment ratio M_c/M_y, plastic rotation in the post-yielding region θ_p, post-capping rotation θ_{pc}, and ultimate rotation θ_u, which are determined based on the regression equations calibrated according to 255 reinforced

concrete column experiments (Haselton et al., 2016). On the other hand, the limit-state material developed by Elwood and Moehle (2005) was implemented to simulate the stiffness and strength degradation caused by the shear failure and loss of axial capacity. The axial and shear springs were accompanied by rotational springs and added to elastic beam-column elements in series. Their behaviors were defined by the limit-state curve available in OpenSees. The shear failure is triggered when the column's total response exceeds the shear limit curve, which comprises the shear capacity V_n, degrading slope K_{deg}, and residual shear strength V_{res} based on experimental data. Similarly, once the response exceeds the axial limit curve, axial failure will be triggered, which tends to occur when the shear strength degrades to approximately zero.

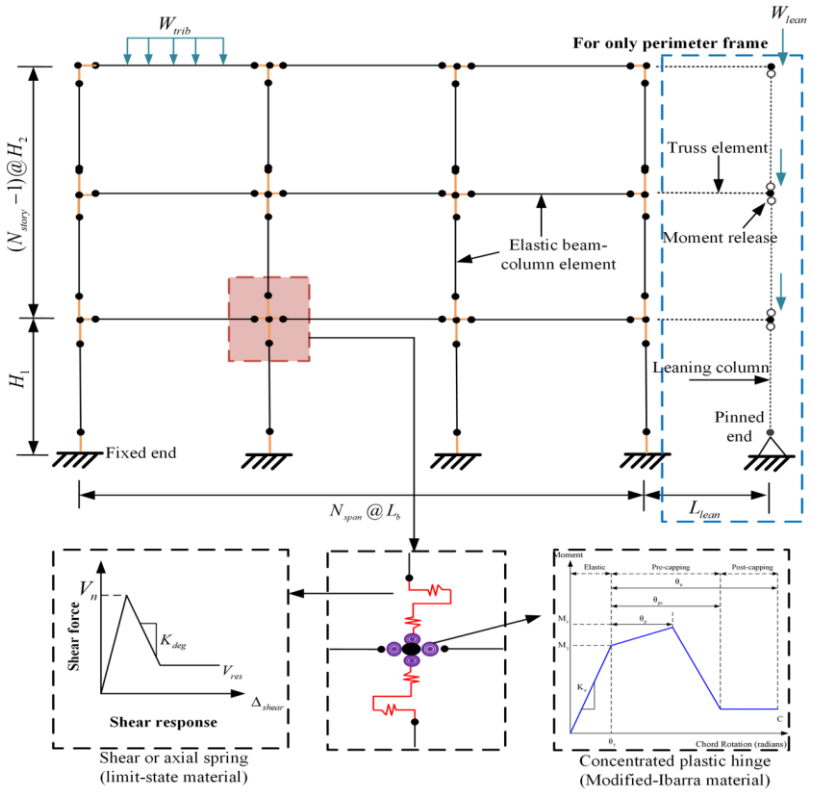

Figure 2. Proposed NDRCB model.

2.2 Validation

To ensure that the auto-modeling procedure can reproduce critical behaviors of the NDRCB frame, cyclic responses of experimental results and dynamic responses from instrumented NDRCB were selected to validate the proposed model. For the cyclic response, prior experimental data of the shear-critical column conducted by Lyn et al. (1996) was also compared, as shown in Figure 3 (a). It is worth mentioning that the post-peak sudden strength loss caused by the shear failure can be reproduced for specimen 3CLH18, which demonstrates that the shear spring in the numerical model works well. In addition, the actual data recorded at the Van Nuys Hotel, a well-known nonductile building, were also used to validate the dynamic response of the proposed model. Figures 3(b) and (c) show the roof acceleration in the east-west direction of the Van Nuys Hotel subjected to the 1992 Big Bear and 1994 Northridge earthquakes. The PGA measured during the 1992 Big Bear earthquake was 0.06 g; therefore, the building most likely remained in the linear region. The maximum response of the proposed model only has a difference of 3% compared with the actual data. While subjected to the Northridge earthquake, the building reached the nonlinear region because PGA was 0.59 g. The difference between the proposed model and the recorded data was approximately 4%. Although a mismatch is expected between the proposed model and the actual data owing to a certain degree of simplification, the proposed model can still capture the critical behavior of NDRCB frames.

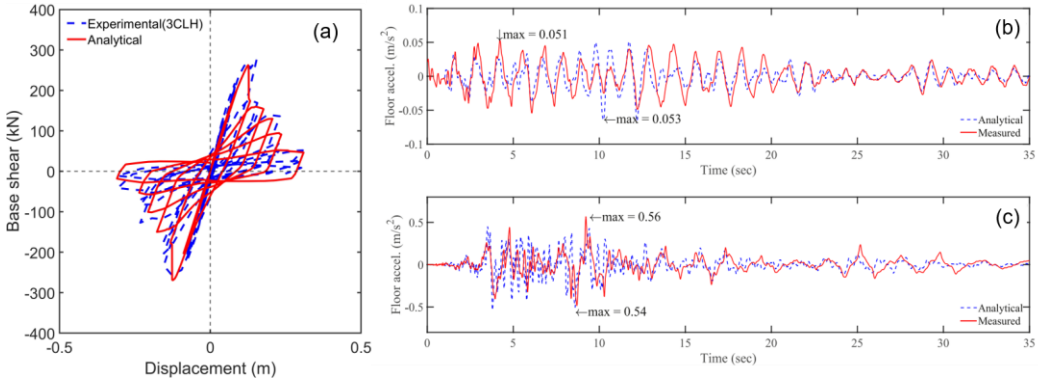

Figure 2. Validation through (a) cyclic analysis and dynamic analysis subjected to (b) the Big Bear earthquake and (c) the Northridge earthquake.

3 Probabilistic assessment

3.1 Probabilistic seismic demand model

The probabilistic seismic demand model (PSDM, Cornell et al., 2002) was selected to construct the damage state fragility functions of NDRCB frames because it has the advantage of being compatible with a closed-form solution and does not require scaling of ground motions. As expressed by Equation (5), a probabilistic curve describing the likelihood that demand *D* exceeds capacity *C* given an intensity level (*IM*) can be constructed through the PSDM. In Equation (5), *a*, *b*, and $\beta^2_{D|IM}$ are the inverse logarithm of the vertical intercept, the slope, and the lognormal standard deviation, respectively. These parameters can be obtained by conducting the linear regression of the logarithmic ground motion intensity and structural response (e.g., peak inter-story drift ratio and peak floor acceleration). β_C and β_M denote the aleatory uncertainty in the capacity and epistemic uncertainty in modeling, respectively, were assumed to be 0.3 and 0.2 based on prior studies (Jeon et al., 2013; Celik et al., 2010).

$$P(D>C|IM)=1-\Phi\left(\frac{\ln\hat{C}-\ln(a\cdot IM^{b})}{\sqrt{\beta^2_{D|IM}+\beta^2_{C}+\beta^2_{M}}}\right) \quad (5)$$

3.2 Soil-structure interaction

As well documented in the literature (Mylonakis et al., 2000), neglecting or oversimplifying the complex dynamic behavior between the structure, its foundation, and the supporting soil media may lead to misleading predictions of superstructure behavior under seismic loading. Hence, this study further considered the soil-structure interaction (SSI) for the proposed NDRCBs. Given the inventory of the NDRCBs located in Los Angeles, the archetypal frames were assumed to be founded on soil profiles categorized as class *D* by NEHRP (Council et al., 1997). The lumped parameter (LP) modeling method (Lesgidis et al., 2015) was adopted to account for the SSI effects. A schematic of the LP model is shown in Figure 3. In the LP method, the shear-wave velocity variability along the soil profile layering was considered through a normal distribution within the range of 180-360 m/s for the NEHRP class *D* soil. The inelastic constitutive law of each soil layer was defined using the shear modulus and material damping curves relative to the soil shear strain. Within each nonlinear dynamic analysis of a building subjected to an earthquake, a bedrock (i.e., fixed foundation) situation was first analyzed. Nonlinear one-dimensional site response analysis was then performed on the randomly generated soil profile based on the variability of class D soil properties for the deconvoluted bedrock ground motion. The results of the site response analysis were then combined with the cone model method (Wolf et al., 2004) to extract the impedance functions and calibrate the LP model.

3.3 Fragility Assessment

To construct the PSDM, nonlinear dynamic analysis was implemented through the proposed modeling of NDRCBs and the selected ground-motion sets to obtain the building responses and intensity measurements for the regression analysis. In this study, the generic suite of ground motions proposed by Baker et al. (2011) was used. The suite consists of four ground motion sets, including far- and near-field records. In the first three

sets, 120 pairs of broadband ground motions with large magnitude and small distance are included: Set 1A ($M_w = 7$, $R_{rup} = 10$ km, soil site); Set 1B ($M_w = 6$, $R_{rup} = 25$ km, soil site); and Set 2 ($M_w = 7$, $R_{rup} = 10$ km, rock site). Set 4 contains 40 pairs of ground motions featuring strong velocity pulses that are expected at near-fault sites or due to directivity effects.

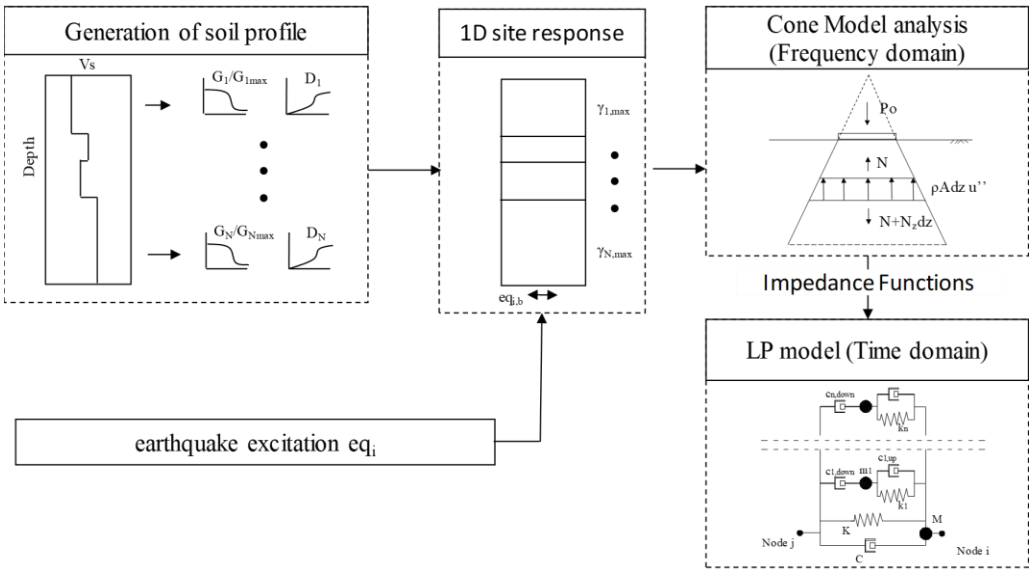

Figure 3. Schematic of the LP model for SSI.

Six archetypal NDRCB models, consisting of three types of building height (i.e., 2-story, 5-story, and 12-story) and two types of frame system (i.e., perimeter frame and space frame) were subjected to 320 ground motions with/without the consideration of SSI to construct the fragility functions. Four damage states (i.e., slight, moderate, extensive, and complete) defined in HAZUS (2003) were adopted to construct the fragility curves. For the low-rise building, the capacity thresholds of the peak story-drift ratio for the four damage states are 0.5%, 0.8%, 2%, and 5%. For the mid-rise building, the capacity thresholds of the peak story-drift ratio for the four damage states are 0.33%, 0.53%, 1.3%, and 3.3%. For the high-rise building, the capacity thresholds of the peak story-drift ratio for the four damage states are 0.25%, 0.4%, 1%, and 2%. Figure 4 and Figure 5 indicate that the consideration of SSI increases the seismic demand for the archetypal frames, which means a lower median intensity to reach the damage threshold. From the fragility curves, it was observed that the seismic demand increased with the height of the archetypal model.

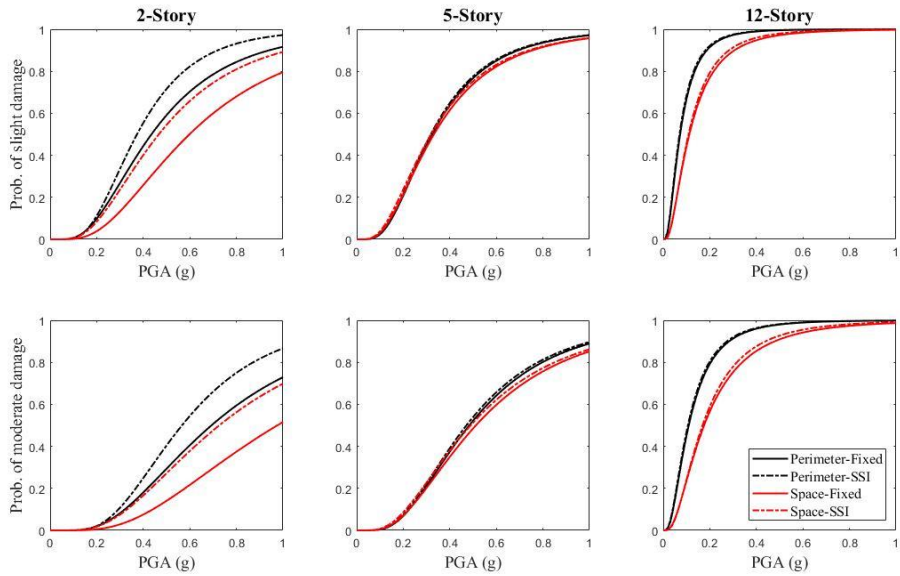

Figure 4. Schematic of the LP model for SSI.

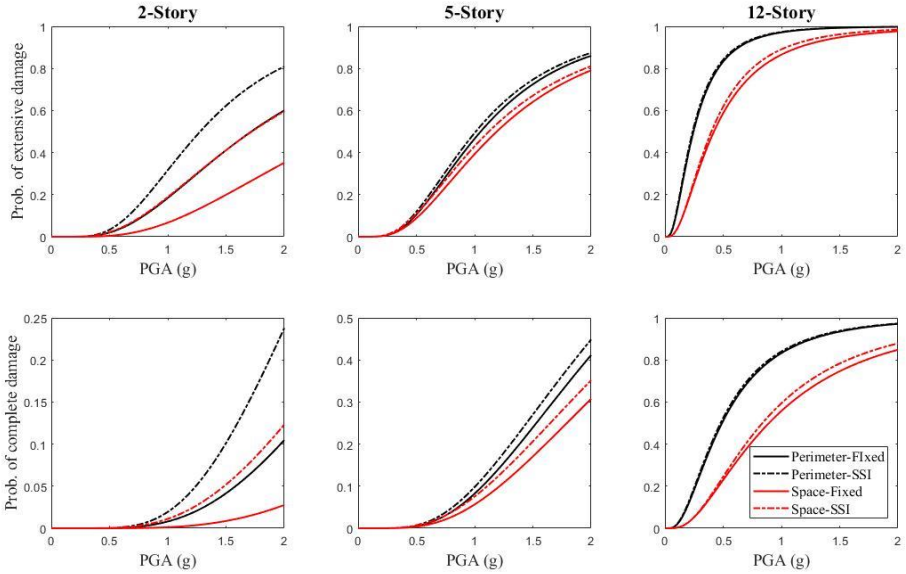

Figure 5. Schematic of the LP model for SSI.

3.4 Optimal intensity measurement

To further illustrate the potential application of the proposed method, the archetypal frames were used to investigate the optimal intensity measurements. Eight IMs were investigated in this study, including the conventional amplitude-based measures (i.e., s_{a,T_1} , s_d , PGA, PGV) and cumulative and duration-based measures (i.e., CAV, I_a , $D_{s,575}$, $D_{s,595}$). Five metrics were selected to evaluate IMs—namely, efficiency, practicality, proficiency, coefficient of determination, and sufficiency. A lower $\beta_{\mathbf{D|IM}}$ in the PSDM represents a smaller variation of the estimated demand for a given IM, thus indicating an efficient IM. The practicality is used to evaluate the dependence of the demand and IM, which can be measured by the slope *b* in the PSDM. If the slope is close to zero, the dependence of the demand and IM can be ignored; therefore, the IM is impractical. Proficiency is a composite measurement of efficiency and practicality, which can be calculated by $\zeta = \beta_{\mathbf{D|IM}} / b$. A lower value of ζ indicates a more proficient IM and lower uncertainty in the demand model by the selection of the IM. The coefficient of determination R^2 can validate the PSDM assumption of the linear relationship in lognormal space. A higher R^2 value indicates the goodness of the regression fit and reduces dispersion among the dataset. A sufficient IM is independent of the ground motion characteristics, such as the magnitude M_w and epicentral distance *R*, which can be evaluated by the statistical *p*-value. If the *p*-value is greater than the significance level (e.g., 5%), then IM is not statistically significant. This means that the independence of the IM and ground motion characteristics holds, and thus, the IM is *sufficient*.

Table 1. Evaluation metrics of IMs for the peak interstory drift ratio.

Intensity Measurements	Efficiency	Practicality	Proficiency		Sufficiency	
	$\beta_{\mathbf{D\|IM}}$	b	ζ	R^2	M_w	R
s_{a,T_1} (g)	0.73	0.71	1.03	0.33	0.0	**0.33**
s_d (cm)	0.68	0.96	0.71	0.62	0.02	0.0
PGA (g)	0.59	**1.05**	0.57	0.46	0.0	0.0
PGV (m/s)	**0.39**	1.0	**0.39**	**0.65**	**0.08**	0.24
I_a (m/s)	0.5	0.68	0.73	0.55	0.0	0.12
CAV (m/s)	1.08	0.34	3.17	0.02	0.0	0.0
$D_{s,575}$ (sec)	1.03	0.19	5.4	0.02	0.0	0.0
$D_{s,595}$ (sec)	1.02	0.35	2.9	0.04	0.0	0.0

As summarized in Table 1, PGV dominated the efficiency, proficiency, R^2, and sufficiency for the peak inter-story-drift ratio. Hence, PGV was recommended as the IM to evaluate the seismic performance of NDRCBs, which is consistent with the prior study (Jeon et al., 2015).

4 Sensitivity analysis

When applying the proposed work to the large-scale seismic assessment of NDRCBs, it is important to identify its sensitivity because it allows users with different levels of knowledge in seismic analysis to input fundamental information about a building. If it is sensitive to the metadata, it may lead to large differences and uncertainties in the evaluation results from different people. Considering that potential users may not precisely provide the building configurations, a deterministic sensitivity analysis was conducted to quantify the variation introduced by the user-provided variables (i.e., first and typical floor height, floor area, span length) in the peak inter-story drift ratio.

The variability of the peak inter-story drift ratio θ_{max} was quantified through the quartile coefficient of dispersion (QCD, Bonett et al., 2006), which is less prone to the outlier influence. The QCD is calculated by (*Q3-Q1*)/(*Q3+Q1*), where *Q3* and *Q1* denote the third and first quartile of the dataset. The QCD was summarized through box plots shown in Figure 6. The results indicated that θ_{max} values for high-rise buildings are relatively sensitive to the user-defined variables compared to low-rise and mid-rise buildings. It must be noted that the sensitivity was investigated, given the condition that users only change basic building configurations instead of the modeling assumptions in the proposed method. The detailing decisions were not investigated because the design procedure only generated two types of sections (i.e., first floor, typical floor) that satisfy the minimum requirement of the UBC of the time. Given this simplification, the archetypal models are believed to be conservative, and the detailing will not vary too much.

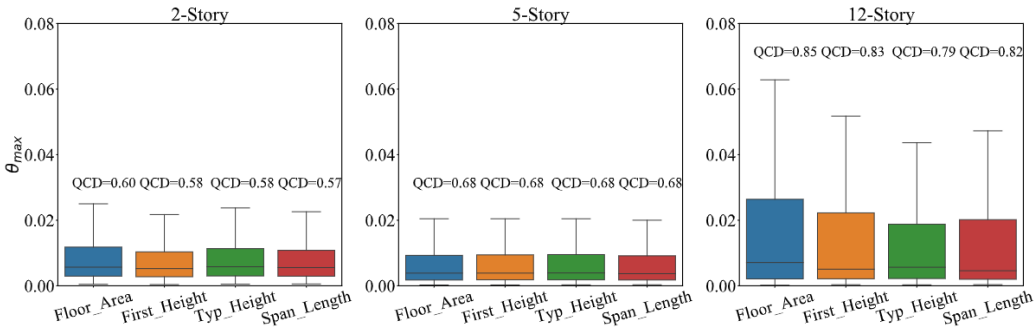

Figure 6. Sensitivity analysis for the peak inter-story drift ratio.

5 Application to residual functionality evaluation

With the presented tool, 1,500 NDRCBs in Los Angeles were efficiently analyzed, and the required assessment time was reduced from months to hours. As a potential application to understanding city resilience, the residual functionality of these buildings was estimated based on their seismic performance level. According to the ASCE (2014), the performance level of a building was defined as immediate occupancy(IO), life safety(LS), and collapse prevention(CP) with the thresholds of 0.5%, 1%, and 2% of peak inter-story drift ratio, respectively. With the performance level, a triangular distribution can then be implemented to incorporate the uncertainties associated with functionality. The lower bound, upper bound, and mode corresponding to IO, LS, and CP were assumed to be (0.7, 0.9, 0.8), (0.4, 0.6, 0.5), and (0, 0.2, 0), respectively (Dong et al., 2013). Figure 7 illustrates the average residual functionality of the NDRCBs when subjected to the selected 320 ground motions. It was observed that more than 60% of the NDRCBs exhibited functionalities less than 50% after an earthquake. This outcome can be further adopted to quantify the recovery time and the corresponding resilience index proposed by Cimellaro et al. (2011).

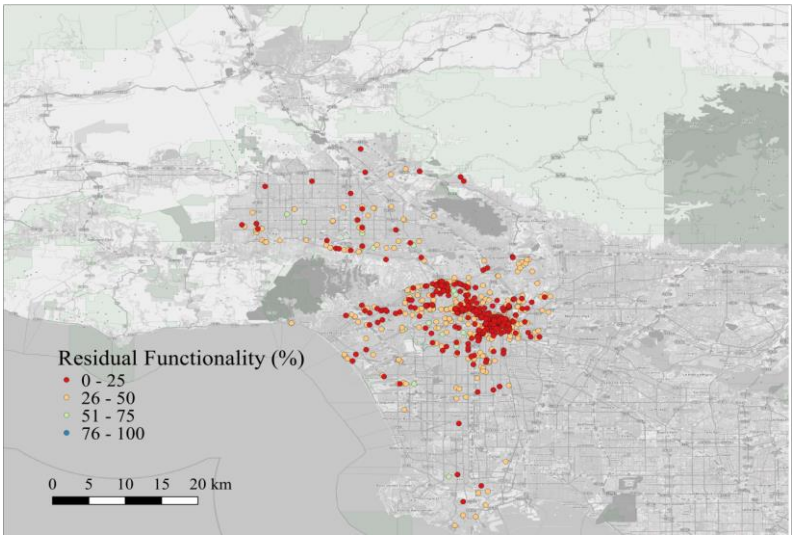

Figure 7. Estimation of the residual functionality of NDRCBs in Los Angeles.

6 Conclusions

In this study, a method for automating the development of nonlinear time-history analysis models and damage fragility functions was proposed for NDRCB frames. Archetypal frames were constructed using basic building metadata and a reverse design procedure that follows the 1967 UBC. Nonlinear elements capable of simulating the stiffness degradation and brittle failure in columns were integrated into the proposed method, and the OpenSees model files were automated and prepared. The method was validated and calibrated through nonlinear cyclic and nonlinear dynamic analyses on previously studied NDRCB frames. A generic suite of ground motions was used to conduct nonlinear time-history analyses of archetypal frames for developing the probabilistic seismic demand model, which was further used to construct the damage fragility curves. The soil-structure interaction effects were simulated by implementing a lumped parameter model while considering the uncertainties in the site soil profiles, which underlined the importance of considering the SSI because it increased both the seismic demands and the uncertainties in PSDM. The efficiency, practicality, proficiency, and sufficiency metrics were investigated to identify the optimal IM. The results indicated that PGV is ideal for capturing the variability in the peak inter-story drift ratio. A deterministic sensitivity analysis was conducted to quantify the variability in the output of the proposed method with respect to uncertainties in building metadata, which indicated that the high-rise archetypal frame was relatively sensitive to the input data compared to other building types. Finally, an application of the proposed method to estimate the residual functionality of NDRCBs in Los Angeles was presented, which highlighted the potential use in large-scale resilience evaluation.

7 Data Availability

Data and codes involved in this study are publicly available on DesignSafe's Data Depot (https://www.designsafe-ci.org/data/browser/public/designsafe.storage.published/PRJ-4038).

8 References

Anagnos, T., Comerio, M.C., Goulet, C., Na, H., Steele, J. and Stewart, J.P., 2008. Los Angeles inventory of nonductile concrete buildings for analysis of seismic collapse risk hazards. In *Proceedings of the 14th world conference on earthquake engineering*.

Applied Technology Council and National Earthquake Hazards Reduction Program (US), 2012. *Seismic performance assessment of buildings*. Federal Emergency Management Agency.

American Society of Civil Engineers., 2013. Minimum design loads for buildings and other structures. American Society of Civil Engineers.

American Society of Civil Engineers, 2014, May. Seismic evaluation and retrofit of existing buildings. American Society of Civil Engineers.

Anagnos, T., Comerio, M.C. and Stewart, J.P., 2016. Earthquake loss estimates and policy implications for nonductile concrete buildings in Los Angeles. *Earthquake Spectra*, *32*(4), pp.1951-1973.

Bonett, D.G., 2006. Confidence interval for a coefficient of quartile variation. *Computational statistics & data analysis*, *50*(11), pp.2953-2957.

Baker, J.W., Lin, T., Shahi, S.K. and Jayaram, N., 2011. New ground motion selection procedures and selected motions for the PEER transportation research program. *PEER report*, *3*.

Council, B.S.S., 1997. NEHRP Recommended Provisions for Seismic Regulations for New Buildings and Other Structures, Part 1 Provisions. *FEMA302*.

Cornell, C.A., Jalayer, F., Hamburger, R.O. and Foutch, D.A., 2002. Probabilistic basis for 2000 SAC federal emergency management agency steel moment frame guidelines. *Journal of structural engineering*, *128*(4), pp.526-533.

Celik, O.C. and Ellingwood, B.R., 2010. Seismic fragilities for nonductile reinforced concrete frames–Role of aleatoric and epistemic uncertainties. *Structural Safety*, *32*(1), pp.1-12.

Comartin, C., Bonowitz, D., Greene, M., McCormick, D., May, P. and Seymour, E., 2011. The Concrete Coalition and the California Inventory Project: An estimate of the number of pre-1980 concrete buildings in the state. *September, Oakland, CA: The Earthquake Engineering Research Institute*.

Cimellaro, G.P., Christovasilis, I.P., Reinhorn, A.M., De Stefano, A. and Kirova, T., 2011. *L'Aquila Earthquake of April 6, 2009 in Italy: Rebuilding a Resilient City to Withstand Multiple Hazards*. MCEER.

Castillo, J.G.S., Bruneau, M. and Elhami-Khorasani, N., 2022. Seismic resilience of building inventory towards resilient cities. *Resilient Cities and Structures*, *1*(1), pp.1-12.

Dong, Y., Frangopol, D.M. and Saydam, D., 2013. Time‐variant sustainability assessment of seismically vulnerable bridges subjected to multiple hazards. Earthquake Engineering & Structural Dynamics, 42(10), pp.1451-1467.

Elwood, K.J. and Moehle, J.P., 2005. Drift capacity of reinforced concrete columns with light transverse reinforcement. *Earthquake Spectra*, *21*(1), pp.71-89.

Haselton, C.B., Liel, A.B., Taylor-Lange, S.C. and Deierlein, G.G., 2016. Calibration of model to simulate response of reinforced concrete beam-columns to collapse. *ACI Structural Journal*, *113*(6).

Ibarra, L.F., 2004. *Global collapse of frame structures under seismic excitations*. Stanford University.

Jeon, J.S., 2013. Aftershock vulnerability assessment of damaged reinforced concrete buildings in California. *Georgia Institute of Technology*.

Jeon, J.S., DesRoches, R., Lowes, L.N. and Brilakis, I., 2015. Framework of aftershock fragility assessment–case studies: older California reinforced concrete building frames. *Earthquake Engineering & Structural Dynamics*, *44*(15), pp.2617-2636.

Lynn, A. C., Moehle, J. P., Mahin, S. A., & Holmes, W. T., 1996. Seismic evaluation of existing reinforced concrete building columns. *Earthquake Spectra*, *12*(4), 715-739.

Liel, A.B., Haselton, C.B. and Deierlein, G.G., 2011. Seismic collapse safety of reinforced concrete buildings. II: Comparative assessment of nonductile and ductile moment frames. *Journal of Structural Engineering*, *137*(4), pp.492-502.

Liel, A.B. and Deierlein, G.G., 2012. Using collapse risk assessments to inform seismic safety policy for older concrete buildings. *Earthquake Spectra*, *28*(4), pp.1495-1521.

Liel, A.B. and Deierlein, G.G., 2013. Cost-benefit evaluation of seismic risk mitigation alternatives for older concrete frame buildings. *Earthquake Spectra*, *29*(4), pp.1391-1411.

Lignos, D. G., & Krawinkler, H., 2013. Development and utilization of structural component databases for performance-based earthquake engineering. *Journal of Structural Engineering*, *139*(8), 1382-1394.

Lesgidis, N., Kwon, O.S. and Sextos, A., 2015. A time domain seismic SSI analysis method for inelastic bridge structures through the use of a frequency-dependent lumped parameter model. Earthquake Engineering & Structural Dynamics, 44(13), pp.2137-2156.

Mylonakis, G. and Gazetas, G., 2000. Seismic soil-structure interaction: beneficial or detrimental? *Journal of earthquake engineering*, *4*(3), pp.277-301.

Mr, H.M., 2003. Multi-hazard loss estimation methodology: Earthquake model. *Department of Homeland Security, FEMA, Washington, DC*, pp.235-260.

Wolf, J.P. and Deeks, A.J., 2004. *Foundation vibration analysis: A strength of materials approach*. Elsevier.